

[P₂S₁₀]⁴⁻: A Novel Polythiophosphate Anion Containing a Tetrasulfide Fragment

Jennifer A. Aitken, Christian Canlas,
David P. Weliky, and Mercouri G. Kanatzidis*

Department of Chemistry and Center for Fundamental
Materials Research, Michigan State University,
East Lansing, Michigan 48824

Received June 21, 2001

Introduction

Polychalcophosphate fluxes are now a well-established tool for preparing new ternary and quaternary thio- and selenophosphates.^{1–4} The in-situ fusion of A₂Q, P₂Q₅, and Q (A = an alkali metal and Q = S or Se) forms highly reactive, discrete [P_yQ_z]ⁿ⁻ fragments solubilized in excess polychalcogenide flux. These anions act as ligands to metal cations, forming solids with structures of every dimensionality. The exact thermodynamic and kinetic processes and speciation equilibria present in these fluxes remains ill understood, and physicochemical studies aimed at understanding them are few. The isolation and identification of new [P_yQ_z]ⁿ⁻ anions will help us better understand the nature of these fluxes and provide some insight into how the various multinary compounds form. Thus far, several alkali metal salts of [P_yQ_z]ⁿ⁻ anions have been structurally characterized, such as [PQ₄]³⁻,⁵ [P₂S₆]²⁻,⁶ [P₂Q₆]⁴⁻,⁷ [P₂Se₉]⁴⁻,⁸ and [P₈Se₁₈]⁶⁻.⁹ Here we report the synthesis and characterization of the novel [P₂S₁₀]⁴⁻ anion, which consists of two PS₄ tetrahedra connected via a disulfide, giving rise to a S₄²⁻ fragment in this anion.

Experimental Section

Syntheses. Cs₂S was prepared by reacting stoichiometric amounts of the elements in liquid ammonia.¹⁰

Single crystals of Cs₄P₂S₁₀ were initially obtained from a mixture of Pb (0.3 mmol), P₂S₅ (0.6 mmol), Cs₂S (0.9 mmol), and S (2.4 mmol) which was heated in an evacuated Pyrex tube to 500 °C for 4 days followed by cooling at 2 °C/h. The residual flux was removed with *N,N*-dimethylformamide, and after washing with ether, yellow needle-like crystals were found. Following a single-crystal structure analysis,

Table 1. Crystallographic Data for Cs₄P₂S₁₀^a

formula	Cs ₄ P ₂ S ₁₀	<i>d</i> _{calc} (mg/m ³)	3.065
fw	914.18	<i>m</i> (mm ⁻¹)	8.492
space group	<i>P</i> 2 ₁ / <i>c</i> (#14)	wavelength (Å)	0.71073
<i>a</i> (Å)	17.386(1)	temp (K)	173
<i>b</i> (Å)	7.1433(4)	2θ _{max} (°)	54.28
<i>c</i> (Å)	24.021(1)	<i>R</i> indices (<i>I</i> > 2σ(<i>I</i>))	R1 = 0.0308
β (°)	95.015(1)		wR2 = 0.0536
vol (Å ³)	2971.8(3)	<i>R</i> indices (all data)	R1 = 0.0515
<i>Z</i>	6		wR2 = 0.0571

$$^a \text{R1} = \sum |F_o| - |F_c| / \sum |F_o| \text{ and } \text{wR2} = \{ \sum [w(F_o^2 - F_c^2)] / \sum [w(F_o^2)] \}^{1/2}$$

we devised a rational synthesis: a mixture of Cs₂S (1.2 mmol), P₂S₅ (0.6 mmol), and S (4.2 mmol)¹¹ was heated in an evacuated Pyrex tube to 500 °C for 2 days followed by cooling at 10 °C/hr. The product was isolated in the same manner as above, yielding pure Cs₄P₂S₁₀, which decomposes in H₂O. Cs₄P₂S₁₀ seems to be stable in air at least for a few days.

Physical Measurements. Powder X-ray diffraction (PXRD) analyses were performed using an INEL CPS120 powder diffractometer (flat geometry) with graphite monochromatized Cu Kα radiation. Differential thermal analyses (DTA) were performed on a Shimadzu DTA-50 thermal analyzer. To assess congruent melting, we compared the X-ray powder diffraction patterns before and after DTA experiments. The stability and reproducibility of the samples were monitored by running multiple heating/cooling cycles. Optical diffuse reflectance measurements were performed at room temperature using a Shimadzu UV-3101PC double beam, double monochromator spectrophotometer.¹² Raman spectra were recorded on a Holoprobe Raman spectrograph equipped with a 633 nm HeNe laser and a CCD detector and coupled to an Olympus BX60 microscope. ³¹P Solid State NMR spectra were obtained on a Varian Infinity Plus spectrometer operating at 398.5 MHz and ambient temperature; 10 kHz spinning was used with a 4 mm Varian magic angle spinning probe. The recycle delay was 3500 s, which is at least two times longer than the longest *T*₁ of any of the observed signals. The chemical shifts are referenced to 85% H₃PO₄ (0 ppm).

X-ray Structure Determination. A Bruker SMART Platform CCD diffractometer, operating at -100 °C and using graphite monochromatized Mo Kα radiation (0.71073 Å), was used to collect data on a single crystal 0.4 × 0.1 × 0.1 mm (Table 1). A hemisphere of data was collected in three major swaths of frames, with 0.30° steps in ω and 30 s/frame exposure. A total of 20 444 reflections were collected, and of those, 6 480 were unique with an *R*_{int} = 0.0464. Data collection and reduction were carried out using SMART and SAINT, an empirical absorption correction was done using SADABS, and the structural solution (direct methods) and all refinements were performed using SHELXTL.¹³ Six cesium atoms, three phosphorus atoms, and fifteen sulfur atoms were located within two rounds of least-squares/difference Fourier cycles; however, two significant peaks remained in the difference Fourier map. These two peaks were assigned as S(14') and S(15') since they generated a tetrasulfide unit which was located very close (<1 Å) to the S(14)–S(15)–S(15)–S(14) chain. No change in the *R* values and little change in the occupancies was noted when the occupancies were refined freely [S(14) = 0.67, S(15) = 0.68, S(14') = 0.31, and S(15') = 0.28] or constrained [S(14) = S(15) = 0.692(4) and S(14') = S(15') = 0.308(4)]. All atoms were subsequently refined

- (1) (a) Kanatzidis, M. G. *Curr. Opin. Solid State Mater. Sci.* **1997**, 2(2), 139–149, and references therein. (b) Aitken, J. A.; Kanatzidis, M. G. *Inorg. Chem.* **2001**, 40, 2938–2939.
- (2) (a) Evenson, C. R., IV; Dorhout, P. K. *Inorg. Chem.* **2001**, 40, 2875–2883. (b) Evenson, C. R., IV; Dorhout, P. K. *Inorg. Chem.* **2001**, 20, 2884–2891.
- (3) Derstroff, V.; Tremel, W. *Chem. Commun.* **1998**, 8, 913–914.
- (4) Gauthier, G.; Jobic, S.; Brec, R.; Rouxel, J. *Inorg. Chem.* **1998**, 37, 2332–2333.
- (5) (a) Mercier, R.; Malugani, J. P.; Fahys, B.; Robert, G. *Acta Crystallogr.* **1982**, 38, 1887–1890. (b) Jansen, M.; Henseler, U. *J. Solid State Chem.* **1992**, 99, 110–119. (c) Schäfer, H. Schäfer, G.; Weiss, A. Z. *Naturforsch* **1965**, 20b, 811.
- (6) Brockner, W.; Becker, R.; Eisenmann, B.; Schäfer, H. Z. *Anorg. Allg. Chem.* **1985**, 520, 51–58.
- (7) Mercier, R.; Malugani, J. P.; Fahys, B.; Douglade, J. Robert, G. *J. Solid State Chem.* **1982**, 43, 151–162.
- (8) Chondroudis, K.; Kanatzidis, M. G. *Inorg. Chem.* **1995**, 34, 5401–5402.
- (9) Chondroudis, K.; Kanatzidis, M. G. *Inorg. Chem.* **1998**, 37, 2582–2584. K₆P₈Se₁₈ is soluble in a solution of crown ether in DMF.
- (10) Feher, F. In *Handbuch der Präparativen Anorganischen Chemie* Brauer, G., Ed.; Ferdinand Enke: Stuttgart, Germany, 1954; pp 280–281.

- (11) Stoichiometric reactions yielded a mixture of Cs₄P₂S₁₀ and what we believe to be Cs₄P₂S₆ as indicated by ³¹P NMR spectroscopy and powder X-ray diffraction. Four extra equivalents of S were determined necessary in order to obtain Cs₄P₂S₁₀ in pure form
- (12) Aitken, J. A.; Marking, G. A.; Evain, M.; Iordanidis, L.; Kanatzidis, M. G. *J. Solid State Chem.* **2000**, 39, 1525–1533.
- (13) SMART, SAINT, SHELXTL V-5 and SADABS; Bruker Analytical X-ray Instruments Inc.: Madison, WI 53719.

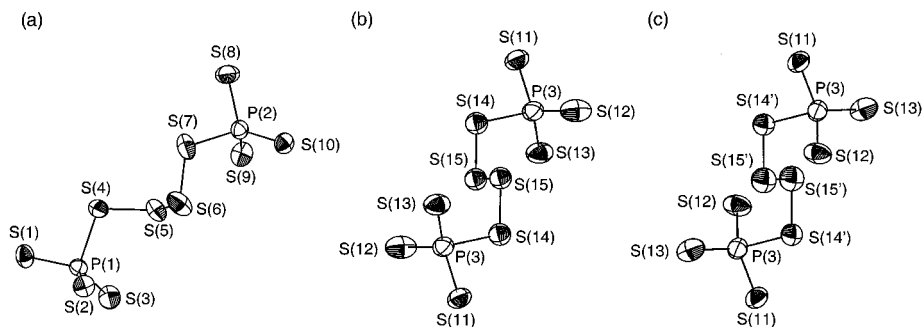


Figure 1. ORTEP (Farrugia, L. J. *J. Appl. Cryst.* **1997**, *30*, 565.) representations (with thermal vibrational ellipsoids at 90%) of each $[P_2S_{10}]^{4-}$ molecule found in $Cs_4P_2S_{10}$ viewed down the central S–S bond: (a) molecule **1**, (b) molecule **2** when the S(14)–S(15)–S(15)–S(14) chain is present, and (c) molecule **2** when the S(14')–S(15')–S(15')–S(14') chain is present.

Table 2. Selected Intramolecular Distances (Å) and Angles (°) for $Cs_4P_2S_{10}$.

Bonding in Molecule 1		Bonding in Molecule 2	
P(1)–S(1)	2.017(2)	P(3)–S(11)	2.021(2)
P(1)–S(2)	2.009(2)	P(3)–S(12)	1.996(2)
P(1)–S(3)	1.999(2)	P(3)–S(13)	1.990(2)
P(1)–S(4)	2.192(2)	P(3)–S(14)	2.195(3)
S(4)–S(5)	2.057(2)	S(14)–S(15)	2.025(3)
S(5)–S(6)	2.069(2)	S(15)–S(15)	2.143(4)
S(6)–S(7)	2.047(2)		
P(2)–S(7)	2.176(2)		
P(2)–S(8)	2.007(2)		
P(2)–S(9)	1.991(2)		
P(2)–S(10)	2.017(2)		
		Non-Bonding in Molecule 2	
		S(14)–S(14')	0.745(5)
		S(14)–S(15')	2.376(6)
		S(15)–S(15')	0.958(5)
		S(15)–S(15')	1.903(6)
		S(14')–S(15)	2.338(6)
Angles in Molecule 1		Angles in Molecule 2	
S(1)–P(1)–S(4)	96.16(8)	S(11)–P(3)–S(14)	94.13(9)
S(3)–P(1)–S(4)	107.55(9)	S(13)–P(3)–S(14)	102.8(1)
S(2)–P(1)–S(4)	107.57(8)	S(12)–P(3)–S(13)	111.9(1)
S(2)–P(1)–S(3)	112.49(9)	S(12)–P(3)–S(14)	113.3(1)
S(1)–P(1)–S(2)	115.36(9)	S(11)–P(3)–S(12)	115.6(1)
S(1)–P(1)–S(3)	115.76(9)	S(11)–P(3)–S(13)	117.0(1)
P(1)–S(4)–S(5)	107.36(8)	P(3)–S(14)–S(15)	107.3(1)
S(4)–S(5)–S(6)	107.86(9)	S(14)–S(15)–S(15)	100.9(2)
S(5)–S(6)–S(7)	105.89(9)		
S(6)–S(7)–P(2)	108.50(9)	*S(14)S(15)S(15)/S(15)S(15)S(14)	0.0(2)
S(7)–P(2)–S(8)	95.34(9)	*S(14')S(15')S(15')/S(15')S(15')S(14')	0.0(2)
S(7)–P(2)–S(9)	107.16(8)		
S(7)–P(2)–S(10)	110.30(9)		
S(9)–P(2)–S(10)	113.15(9)		
S(8)–P(2)–S(10)	113.83(9)		
S(8)–P(2)–S(9)	115.31(9)		
*S(4)S(5)S(6)/S(5)S(6)S(7)	89.6(2)		
*dihedral angles			
		S(11)–P(3)–S(14')	93.8(2)
		S(13)–P(3)–S(14')	119.7(2)
		S(12)–P(3)–S(14')	96.3(2)
		P(3)–S(14')–S(15')	108.4(3)
		S(14')–S(15')–S(15')	99.4(4)

anisotropically. The maximum and minimum peaks on the final difference Fourier map corresponded to 1.022 and $-1.316 e^{-\text{Å}^{-3}}$.

Results and Discussion

The structure of $Cs_4P_2S_{10}$ consists of $[P_2S_{10}]^{4-}$ anions separated by Cs^+ counterions, which are surrounded by at least eight sulfur atoms that form unusual coordination polyhedra. Each $[P_2S_{10}]^{4-}$ molecule is composed of two PS_4 distorted tetrahedra, which are connected by two sulfur atoms such that a tetrasulfide fragment is formed in the center of the molecule. There are two crystallographically unique $[P_2S_{10}]^{4-}$ molecules in the structure. Looking down the central S–S bond of each shows that they possess different conformations. The tetrasulfide chain of molecule **1** has a dihedral angle of 89.6° while that of molecule **2** is 0° , see Figure 1a and b and Table 2. Molecule **2** has a disordered chain in its center ($\sim 70\%$ occupancy for S(14)–S(15)–S(15)–S(14) and $\sim 30\%$ for S(14')–S(15')–S(15')–S(14')). There is only a 1.6° angle between the planes containing the chains, therefore, either chain gives molecule **2**

the same basic conformation, see Figure 1b and c. The S–S bond lengths in molecule **1** are relatively consistent (2.057(2), 2.069(2), and 2.047(2) Å), whereas those in molecule **2** clearly show a conjugation effect (2.025(3), 2.143(4), and 2.025(3) Å). This discrepancy is due to the different dihedral angles. An S_i-S_j bond length–dihedral SS_iS_j/S_iS_jS angle relationship has been suggested by Hordvik and has been presented graphically as a curve, where the smallest S_i-S_j bond lengths occur for a dihedral angle of 90° while the longest bond lengths correspond to small dihedral angles. The difference in bond lengths is assumed to be partly due to lone pair repulsion, which is most pronounced when the dihedral angle is 0° , and partly due to π bonding, which is most pronounced when the dihedral angle is 90° .¹⁴

The S–P–S bond angles reveal a distortion of the $[PS]_4$ tetrahedra and range from $93.8(2)$ to $119.7(2)^\circ$, with an average S–P–S bond angle of $109.1(2)^\circ$ for P(1), $109.2(2)^\circ$ for P(2),

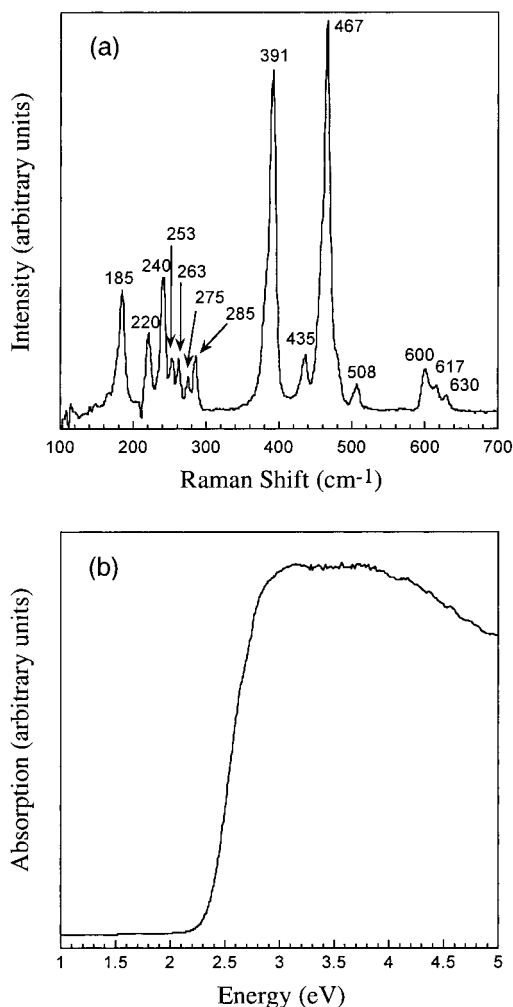


Figure 2. (a) Raman spectrum of $\text{Cs}_4\text{P}_2\text{S}_{10}$. (b) Optical diffuse reflectance spectra converted to absorption for a polycrystalline sample of $\text{Cs}_4\text{P}_2\text{S}_{10}$.

and $109.1(2)$ or $109.1(4)^\circ$ for P(3) when S(14) or S(14') is present. The P–S distances in the $[\text{P}_4\text{S}_{10}]^{4-}$ molecules range from $1.990(2)$ to $2.204(5)$ Å, with average P–S distances of $2.054(4)$ Å for P(1), $2.048(4)$ Å for P(2), and $2.051(5)$ or $2.053(6)$ Å for P(3) when S(14) or S(14') is present. P(1) is displaced 0.194 Å from the center of its tetrahedron, while P(2) and P(3) are displaced 0.183 and 0.210 Å/ 0.237 Å (when S(14)/(S14') is present). The average terminal P–S distances are measurably shorter ($2.005(6)$ Å) than the average P–S distances that serve to connect the P atoms to the $[\text{S}_4]^{2-}$ chains ($2.192(6)$ Å). Although it is more pronounced in this case due to the rather long $[\text{S}_4]^{2-}$ chain, this trend has been observed for other thiophosphate ligands containing terminal and bridging sulfurs.^{15–19} M_2PS_{10} ($\text{M} = \text{V}$,¹⁷ Nb ¹⁸) contains the $[\text{P}_2\text{S}_8]^{4-}$ anion,

which has a disulfide unit in its center and average terminal and bridging P–S distances of $2.014(5)$ and $2.127(3)$ Å for $\text{M} = \text{V}$ and $2.023(3)$ and $2.107(2)$ Å for $\text{M} = \text{Nb}$. $\text{Nb}_4\text{P}_2\text{S}_{21}$ ¹⁹ contains the $[\text{P}_2\text{S}_9]^{4-}$ anion, which contains a trisulfide unit and average terminal and bridging P–S distances of $2.026(3)$ and $2.117(2)$ Å.

The Raman spectrum of $\text{Cs}_4\text{P}_2\text{S}_{10}$ is quite complicated, see Figure 2a. It is difficult to unambiguously assign all of the Raman peaks since expected vibrations for PS_4 and S_4^{2-} fragments overlap in certain regions. By comparison to other PS_4 containing compounds,^{15,16} the peaks at 630 , 617 , and 600 cm^{-1} can be tentatively assigned to P–S, although they are shifted to slightly higher cm^{-1} , probably due to the shorter terminal P–S bonds in the tetrahedra. The three peaks at 508 , 467 (which has a shoulder on both sides), and 435 cm^{-1} can be attributed to S–S stretching of the S_4^{2-} fragment by analogy with K_2S_4 ²⁰ (485 , 478 , 434 cm^{-1}). The very strong peak which occurs at 391 cm^{-1} should be due to the locally A_1 symmetric stretching of the PS_4 tetrahedral unit by analogy with $\text{K}_2\text{CuP}_3\text{S}_9$ ¹⁵ (391 cm^{-1}), K_2AuPS_4 ¹⁶ (395 cm^{-1}), or Cs_2AuPS_4 ¹⁶ (398 cm^{-1}). The peaks below 300 cm^{-1} can be assigned to S–S–S or S–P–S bending modes that occur at similar wavenumbers. This spectrum should prove to be useful in distinguishing the $[\text{P}_4\text{S}_{10}]^{4-}$ anion from other thiophosphate anions.

The optical diffuse reflectance spectrum was obtained for a ground polycrystalline sample of $\text{Cs}_4\text{P}_2\text{S}_{10}$. The compound exhibits a well-defined energy gap, E_g , of ~ 2.4 eV (~ 517 nm), see Figure 2b. DTA, and PXRD analysis before and after DTA, shows that $\text{Cs}_4\text{P}_2\text{S}_{10}$ melts congruently at ~ 420 °C.

Isotropic ^{31}P NMR peaks were observed at 111.1 , 110.3 , and 106.6 ppm. The 106.6 ppm peak also contained a shoulder at 107.5 ppm. The ratio between the total integrated intensity of the 111.1 and 110.3 ppm peaks and that of the 106.6 ppm peak is 2.1 ± 0.2 . These intensity data are consistent with the assignments of the 111.1 and 110.3 ppm peaks to P(1) and P(2) and the 106.6 ppm peak to P(3). Observation of a shoulder for the 106.6 ppm peak is consistent with the disorder observed in the crystal structure for the tetrasulfide chain in the molecules containing P(3).

The exploration of A–P–Q phases is incomplete, and further investigations are warranted since the discovery of new A–P–Q phases containing new or known $[\text{P}_n\text{Q}_m]^{n-}$ anions will help us better understand the nature of polychalcophosphate fluxes. Furthermore, A–P–Q phases may be useful as starting materials for solid-state reactions²¹ or good starting materials for developing the solution coordination chemistry of these potential ligands.⁹

Acknowledgment. Financial support from the National Science Foundation and the use of the W. M. Keck Microfabrication Facility at Michigan State University, a NSF MRSEC facility, are greatly acknowledged. D.P.W. would like to thank the Camille and Henry Dreyfus Foundation for a new faculty award.

Supporting Information Available: An X-ray crystallographic file, in CIF format. This material is available free of charge via the Internet at <http://pubs.acs.org>

IC010664P

- (15) Hanco, J. A.; Sayettat, J.; Jobic, S.; Brec, R.; Kanatzidis, M. G. *Chem. Mater.* **1998**, *10*, 3040–3049.
 (16) Chondroudis, K.; Hanco, J. A.; Kanatzidis, M. G. *Inorg. Chem.* **1997**, *36*, 2623–2632.
 (17) Brec, R.; Ouvrard, G.; Evain, M.; Grenouilleau, P.; Rouxel, J. J. *Solid State Chem.* **1983**, *47*, 174–184.
 (18) Brec, R.; Grenouilleau, P.; Evain, M.; Rouxel, J. *Rev. Chim. Minér.* **1983**, *20*, 295–304.
 (19) Brec, R.; Evain, M.; Grenouilleau, P.; Rouxel, J. *Rev. Chim. Minér.* **1983**, *20*, 283–294.

- (20) Janz, G. J.; Coutts, J. W.; Downey, J. R.; Roduner, E. *Inorg. Chem.* **1976**, *15*(8), 1755–1758.
 (21) Melting points for Na_3PS_4 , $\text{K}_2\text{P}_2\text{S}_6$, $\text{K}_6\text{P}_8\text{Se}_{18}$, $\text{Cs}_2\text{P}_2\text{S}_6$, $\text{Cs}_4\text{P}_2\text{Se}_9$, and $\text{Cs}_4\text{P}_2\text{S}_{10}$ are relatively low and fall in the range of 420 – 520 °C.